

## Quality assurance in the FMI Doppler Weather Radar Network

Elena Saltikoff, Asko Huuskonen, Harri Hohti, Jarmo Koistinen and Heikki Järvinen

*Finnish Meteorological Institute, P.O. Box 503, FI-00101 Helsinki, Finland*

*Received 3 Sep. 2009, accepted 13 Oct. 2009 (Editor in charge of this article: Hannele Korhonen)*

Saltikoff, E., Huuskonen, A., Hohti, H., Koistinen, J. & Järvinen, H. 2010: Quality assurance in the FMI Doppler Weather Radar Network. *Boreal Env. Res.* 15: 579–594.

The Finnish Meteorological Institute designed, acquired and installed a network of 8 C-band Doppler radars during the years 1993–2005. We describe the principles used in the network design, the basic infrastructure of the network, as well as the technical properties of the radars. Data quality is improved by filtering of unwanted echoes and thresholding, and the electrical calibration of power and the antenna pointing is controlled by paired-radar analysis and solar observations. The radar data are used to serve society in a wide range of applications from aviation weather service to flood protection. High quality of end-user products is achieved by maintaining optimal measurements of individual radars, homogeneity of the entire radar network, and careful processing of the data. Volume scans consisting of 11 elevation angles have been designed to give simultaneously good quality precipitation data near the surface, secondly, good quality wind profiles based on the Doppler data, and thirdly, three-dimensional data (cloud tops and cross sections) for the requirements of aviation. Doppler-filtering, image processing and adjustment for vertical profile of reflectivity are applied to improve the data quality.

### Introduction

Meteorological and hydrological communities use weather radars to observe precipitation-related weather phenomena due to the outstanding temporal and spatial resolution achieved with radar measurements.

The basic observables of weather radars are the microwave scattering intensity, phase shift and polarization. In meteorology and its applications, the interest is on the question “what is the 3-dimensional state of the atmosphere that produces the measured values for the observables?” Inversion theoretical approach (e.g., Kaipio and Somersalo 2005) combined with a weather model provides a way to convert the measured values into the desired weather parameters, such as pre-

cipitation intensity or wind velocity. In practice, however, the weather parameters are processed from the direct measurements using physical equations and empirical relationships with rather significant assumptions and compromises (e.g. Battan 1973: 29–62, 145–154; Doviak and Zrnic 1993: 125–140, 160–207, 304–316; Bringi and Chandrasekar 2001: 274–293, 567–569).

Radar data are used in a multitude of precipitation-related applications, because it provides a better resolution in space and time than any other current data source. Typically, radar data are available in a grid of 1 km with a vertical resolution varying between 0.2 to 5 km at time intervals of 5 minutes. This resolution is essential for observing rapidly developing meso-scale weather phenomena such as thunderstorms. In

contrast, synoptic scale weather phenomena, such as cold fronts in the mid-latitudes, are too large to be observed with a single radar although they generate large amounts of precipitation. This highlights an essential feature of radar observations and, in fact, that of all meteorological observations, namely the need for networking. A wide range of scales of atmospheric phenomena can be observed with a homogenous network of radars, which supports many applications such as operational weather monitoring and nowcasting.

This paper describes the design and the use of the single polarization Doppler C-band weather radar network in Finland, constructed during the years 1994–2005. This network is a component in the national weather service infrastructure, aimed primarily at the needs of short-term weather forecasting and nowcasting, but it has also proved to be beneficial for various applications in hydrology, climatology and numerical weather prediction. Special attention is paid in this article to the process of quality assurance which seeks the high quality of measurements of individual radars, the homogeneity of the entire radar network, and the compatibility with adjacent networks in neighbouring regions. The paper illustrates two applications which highlight different needs for quality assurance. In nowcasting, removal of non-precipitating echoes is important. In forest fire warning, any bias in quantitative precipitation estimation is detrimental, as precipitation totals are accumulated and compared with evaporation data from other sources. A bias may lead to unnatural drying or moistening of the forests in the monitoring system, and thus to too many or too few warnings.

## Network design

Designing a weather radar network for a country of the size of Finland (roughly 1200 km north to south, 600 km east to west) is a process involving several spatial scales. The largest of these is the international scale: FMI was one of the founding members of the Nordic Weather Radar Network, (NORDRAD; Carlsson 1994) and the need for data exchange and compositing with the Swedish, Norwegian and Danish radars via NORDRAD has been an essential element of

the network planning from the very beginning. Next, the national scale requires a comprehensive coverage for hydro-meteorological purposes for the total area of the country. The aviation weather service has specific requirements of three-dimensional data, but they concentrate in certain areas only. Finally, on the local scale, favourable sites for radar towers provide high quality measurements in open landscape with an unobstructed horizon, but require an adequate infrastructure and absence of potential sources of interference in the immediate vicinity.

Almost all of Finland — apart from the northernmost Lapland — is covered by radar measurements, provided the data are taken out to the maximum measurement range of 250 km (Fig. 1). A careful placing of the radars, making use of the relatively flat topography of the country has helped to create a network with no major gaps due to beam blocking by terrain, buildings or other obstructions. The radars near the south coast, Korpo and Vantaa, are situated 61 and 81 m above the mean sea level, the Luosto radar in Lapland is at the height of 532 m, and all the others are at heights between these (Table 1).

The shortest distance between any two radars in the network is between Vantaa and Anjalankoski, 145 km. In general, the southern radars are placed less than 200 km from each other. In the north, the distance of 265 km between Utajärvi and Luosto is the longest in the network.

Typical C-band weather radars have antennas with half-power beam widths near  $1^\circ$ . Thus, if the lowest nominal elevation is  $0.5^\circ$ , the lower edge of the beam follows an elevation of  $0^\circ$ . On a plane with no refraction, the beam would follow the surface of the Earth. In the real atmosphere, the spherical shape of the globe makes the beam rise, but the gradient of refractivity partly compensates this effect, and as result, in the ICAO standard atmosphere the beam rises with distance following approximately a curvature radius  $4/3$  times the Earth's radius (*see e.g.* Rinehart 1997: 60, or Battan 1973: 24).

Usually, the radar coverage is calculated from the height of the centre of the beam. Applying a typical lowest elevation angle of  $0.5^\circ$ , the beam reaches the height of 1 km at the distance of 72 km from the radar, the height 2 km at 120 km and that of 5 km at the distance of 250 km. If

one would demand data at or below 1 km everywhere in Finland, the radars should be placed at the intervals of 140 km.

Like other atmospheric instruments, weather radars must be sited with care as bad measurement location can severely corrupt the data. A radar gives the best three-dimensional image of the atmosphere at distances approximately 5 to 50 km from the antenna. Hence, it is beneficial to site radars outside airports. In the era of analog radars, the images of reflectivity patterns could only be seen on the local display, and thus the radars were often located at the major airports in the proximity of the aviation forecasters. Digitalization and automation, and modern data network, have enabled more favourable radar siting and unmanned operation.

## Technical properties

For weather radars, three frequency bands are generally used. The X-band frequency is roughly 9.7 GHz, the C-band frequency 5.6 GHz and the S-band frequency is just below 3 GHz. These correspond to wavelengths of 3 cm, 5.3 cm and 10 cm, respectively (WMO 2006).

The previous generation of weather radars in Finland operated in the X-band and were acquired during the 1980s (King 1989). With these radars, the signal attenuation due to rain and the ground clutter were quite problematic. This experience led to the decision that the upgraded network should operate at the C-band and in the Doppler mode. The Doppler capacity would be used for clutter removal and the longer wavelength would make the data less prone to

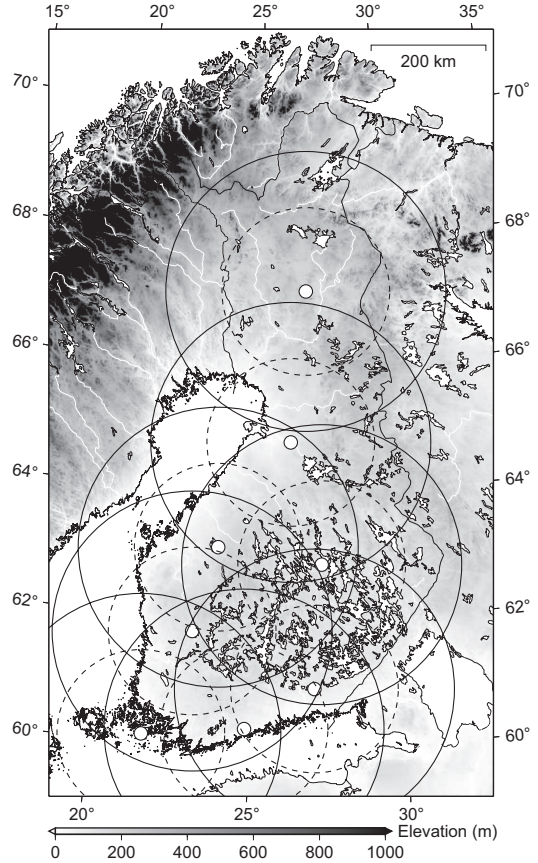


**Fig. 1.** The position of the FMI radars on a topographic map of Finland. The maximum coverage range of 250 km is plotted as a circle around each radar site.

rain attenuation. The original plan was to use the Doppler data primarily for clutter cancellation, and secondarily for wind measurements, processed as vertical profiles of horizontal wind.

The eight radars of the FMI radar network were acquired during a period of 12 years and

**Table 1.** The FMI radar network. Name and three-letter acronym, the start date of operation, the latitude and longitude of the radar and the height of the center of the antenna above mean sea level.

Name	Acronym	Start date	Lat. N	Long. E	Height (m)
Ikaalinen	IKA	15 June 1994	61.7671	23.0799	154
Anjalankoski	ANJ	5 Apr. 1994	60.9036	27.1111	139
Kuopio	KUO	15 Dec. 1995	62.8624	27.3854	268
Korpo	KOR	15 Aug. 1997	60.1284	21.6465	61
Luosto	LUO	1 Aug. 2000	67.1386	26.9008	532
Utajärvi	UTA	26 Sep. 1997	64.7745	26.3225	118
Vantaa	VAN	23 Mar. 1994	60.2706	24.8725	83
Vimpeli	VIM	1 Sep. 2005	63.1046	23.8246	198

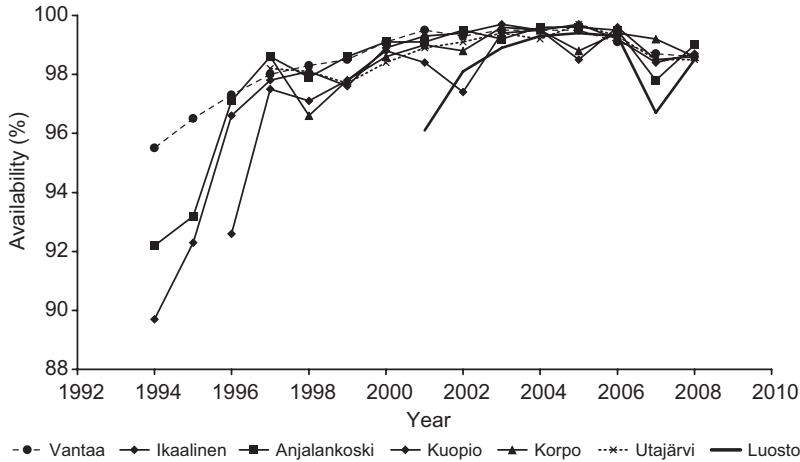


**Fig. 2.** Availability of the FMI radars 1994–2008.

the radars differ slightly in their technical properties (Table 2). The first six radars are practically identical, whereas the two newer ones are different in many details. The northernmost radar in Luosto is a special case for two reasons: in the region of a cold atmosphere and shallow precipitation, a narrow beam with a good vertical resolution is beneficial. The narrow beam also enables 2–3 dB higher gain than with the other radars which helps detecting e.g. weak snowfall frequently occurring in the climate of northern Finland. In addition to the operational weather service, this radar was planned for use in various research projects. It has provided experimental data, e.g., in novel research to solve the range-velocity dilemma (Pirttilä *et al.* 2005).

The data availability is a critical operational measure of the quality of a radar network. At FMI, the data availability is measured by counting how many single radar images are available for the international NORDRAD composite. The availability is 100%, if images arrive from all

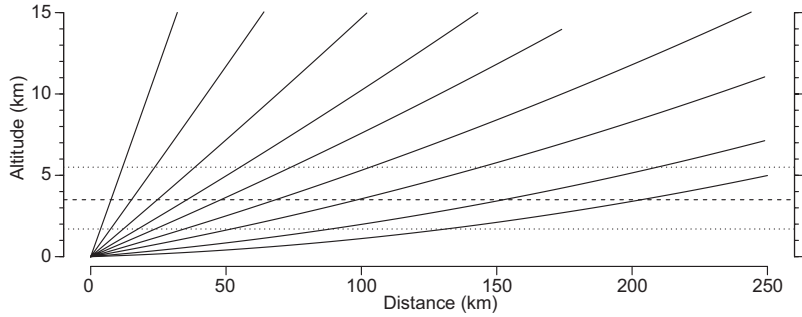
8 radars every 15 minutes within 30 minutes from the nominal measurement time. The figures discussed here contain all regular maintenance breaks and disturbances caused by infrastructure (e.g. power supply and telecommunications) as well as those due to any system malfunctions. During 1997–2008, the annual FMI average was between 98.0% and 99.4%, the best years being 2003–2006, with the availability always above 99.3%. The yearly data availability for each radar (Fig. 2) shows a typical pattern, where the availability increases during the first few years of operations and then starts to decrease slowly after approximately 10 years.

The availability of radar data does not depend only on the radar itself, but also on the infrastructure's ability to provide electricity and continuous data traffic. In some areas, such as Catalonia, Spain, remote radars are equipped with power generators (J. Bech pers. comm.). In Finland, the electrical infrastructure is such that breaks in electricity longer than 15 minutes are

**Table 2.** Technical properties of the radars.

Parameter	VAN, IKA, ANJ, KOR, UTA, KUO	LUO	VIM
Manufacturer	SELEX-SI/Sigmat	SELEX-SI/Sigmat	SELEX-SI/Sigmat
Radar system/processor	Meteor 360C/RVP6	Meteor 500C/RVP8	Meteor 500C/RVP8
Wavelength	5.31–5.35 cm	5.34 cm	5.32 cm
Antenna gain	44.2–45.1 dBi	47.5 dBi	45.0 dBi
Beam width	0.94°–0.98°	0.70°	0.94°
Pulse duration	0.84 $\mu$ s, 2 $\mu$ s	0.5–2 $\mu$ s	0.5–2 $\mu$ s
Transmitted peak power	250 kW	250 kW	250 kW

**Fig. 3.** The height of radar data as a function of the distance from the radar site for the elevation angles used in 1994–2007. The dashed lines represent the median and the 25% quartiles of the heights of the tops of precipitating clouds in Finland.



very uncommon. Thus, it is seen as sufficient to rely on the national power grid, and be prepared for short breaks only by equipping each radar with an uninterruptable power supply (UPS) system, capable of running the radar independently for up to 15 minutes. In case of interruptions in the data transmission, the data are stored on the hard disk of the local computer, and transmitted to the FMI HQ processing centre, as soon as the network connection is again available.

## Measurement program

There is no universal solution for the best measurement program of a radar network. Rather, the solution depends on the hardware, infrastructure, climate and various radar user requirements.

Finland has a single weather radar network with national coverage, which has to fulfill the needs of hydro-meteorology, aviation meteorology and public weather service, as well as several applications related to snowfall. Due to its large land area, and the relatively low number of inhabitants in Finland, the per-capita cost of more than one network would be too high. A different approach has been selected, e.g. in the USA, where two networks co-exist: a terminal Doppler weather radar (TDWR) network for the aviation and the Nexrad (Next generation radar) network for all the other needs (Serafin and Wilson 2000). In France, on the other hand, the measurements of the national network are designed primarily for the needs of hydrology (Tabary 2007).

For the weather service requirements, good vertical resolution is most valuable near the height of the tops of precipitating clouds. Even

though in some cases of severe convection, tops up to 16 km have been observed, statistics in Finland for the year 2007 show the median cloud top height at 2500 m, first quartile at 1700 m and 3rd quartile at 5500 m (Fig. 3). These figures manifest the cold climate of Finland.

Based on the data user-requirements and the possibilities of the radar control software, a measurement task schedule was designed in 1994 to consist of 11 elevation angles, subdivided into three groups (Fig. 3). The radar tasks are controlled using the IRIS (Interactive Radar Information System) software (Sigmet 1997a) which allows the user to configure groups and subgroups of PPI scans with different elevations. Within each group, the basic settings, pulse-repetition frequency, pulse width and data quality measures, are identical, but they differ from one group to the next. These measurement tasks were designed, firstly, to give good quality precipitation data near the surface, secondly, good quality wind profiles based on the Doppler data, and thirdly, reasonable three-dimensional data (cloud tops and cross sections) for the requirements of aviation.

The detailed description of measurement tasks is in Table 3. The first group consisted of four elevation angles, starting from  $0.5^\circ$  and incremented with the nominal beam width of  $1^\circ$ , thus aiming at measuring comprehensively the lowest part of the troposphere. A maximum range of 250 km was agreed within the NOR-DRAD, and it dictated the pulse repetition frequency (PRF) to be 570 Hz, which in turn set the maximum unambiguous velocity interval to  $\pm 7.6 \text{ m s}^{-1}$ . Even though this speed interval is too narrow for useful wind measurements, it is good enough for an effective Doppler filtering.

The 2- $\mu$ s pulse (longer of the two available pulse widths) was used for higher sensitivity.

The second and third groups were scanning higher elevation angles with higher PRFs, and, after year 2005, using dual-PRF velocity unfolding (Joe and May 2003). Large PRF has two advantages: unambiguous velocity range increases and the measurement takes less time. The disadvantage is a smaller unambiguous range, but at higher elevations the radar beam reaches the upper limit of measurement volume (16 km) before reaching the maximum horizontal range. Shorter pulses (1  $\mu$ s or less) had to be used because of the limits of maximum average power output of the magnetron transmitter.

All three groups were repeated every 15 minutes, and the lowest four elevations every 5 minutes.

In 2007, the measurement tasks were changed radically. The reasons were, on one hand, increasing user-requirements for unambiguous Doppler data, and on the other hand, the increased opportunities for controlling each elevation angle separately. Earlier, the Doppler data were used primarily for clutter cancellation, where it is sufficient to know whether a target has a zero or non-zero speed. Another use was the VVP wind profile processing (Waldteufel and Corbin 1979), in which de-aliasing techniques can be used effi-

ciently. Gradually, new user requirements led to the renewal of the measurement tasks to supply un-aliased radial velocities. This serves mainly data assimilation in numerical weather prediction models (Järvinen *et al.* 2009, Salonen *et al.* 2009), and the identification of tornadoes and other intense small-scale weather phenomena. Also several applications needed three-dimensional data at every 5 minutes, instead of 15 minutes. Basic properties of the new task set are given in Table 4. Groups A and B were repeated every 5 minutes, and the other groups executed once or twice during a 15 minutes cycle.

In 2007, the measurement tasks were modified so that more and higher elevation angles were measured every 5 minutes.

## Data quality

### Settings of the radar measurement

The radar software offers a number of parameter settings, which control the processing of the data in the signal processor. By far, the most important of these are related to the treatment of ground clutter. The others determine averaging and resolution, which in turn affect file sizes and how long each measurement task takes.

**Table 3.** Typical basic parameters of the operational measurement tasks during 1994–2007. Small adjustments of the elevation angles were made during the years at different sites. During the first ten years, only single PRFs were used, resulting in smaller maximum velocities (given in parenthesis).

	Elevation angle (deg)	Pulse width ( $\mu$ s)	PRF (Hz)	Number of samples	Range (km)	$V_{\max}$ (m s <sup>-1</sup> )	Repeated (min)
VOL_A	0.3, 0.8, 1.7, 2.7	2 (long)	570	32	250	7.6	5
VOL_B	4, 5.5, 8	1 (short)	850/567 (850)	16	175	22.5 (11.2)	15
VOL_C	13, 25	1 (short)	1200/800 (1200)	16	100	31.8 (15.9)	15

**Table 4.** The basic parameters of the operational measurement tasks during 2007–2009.

	Elevation angle (deg)	Pulse width ( $\mu$ s)	PRF (Hz)	Range (km)	$V_{\max}$ (m s <sup>-1</sup> )	Repeated (min)
PPI A & B	0.3, 1.5, 3, 5, 9	2	570	250	7.6	5
Group C	2	2	570	250	7.6	15
Group D	7, 11	1	675/900	166	35.8	15
Group E	15, 25, 45	1	900/1200	125	48	15
Group F	6, 4, 2	1	600/900	150	23.9	7.5
Group G	0.5	2	427/570	250	22.7	7.5

The ground clutter can be identified in the Doppler radar data because ground targets have near zero velocities. From the Doppler spectrum of radial velocity it is possible to remove the scattered power-related to non-moving targets. The most common methods are based on high-pass filtering of the sampled signal. In case of overlapping weather and clutter echoes (e.g. rain on hills) the removal leads to underestimation of the reflectivity. The more advanced Doppler filtering methods based on spectral processing include algorithms to compensate for the power loss (Passarelli *et al.* 1981, Sigmet 1997b).

Two parameters can be used to adjust the Doppler filtering: one determines the spectral width of ground clutter band and the other one the method used for compensation of underestimation of reflectivity caused by rain with near-zero radial velocities. FMI makes use of wider bands at lower elevations and in more clutter-prone locations. The available processing methods are different for different radars due to different signal processors (Table 2).

Radar data processing takes place in polar coordinates. The antenna moves constantly in the azimuthal direction, so that each pulse is sent in a slightly different azimuthal direction, separated typically by  $0.01^{\circ}$ – $0.05^{\circ}$ . Pulses in a determined sector are processed together. At FMI, this azimuthal resolution is set to be  $1^{\circ}$ , which matches the beam width. The number of pulses processed together (samples) varies between 16 and 64, and together with the pulse repetition frequency this determines the highest possible angular velocity of the antenna. The resolution in the direction of the radial coordinate is determined by splitting the arriving signal into slices called bins. At FMI, processing is carried out in rather short-range bins of 125 m, but then four bins are averaged for output files to decrease the data file sizes. The benefit of this is, that if a single bin is damaged by clutter, the surrounding bins can compensate for this.

In addition to the Doppler filtering, the signal processor software offers methods for thresholding entire bins. The thresholding criteria used for the reflectivity are the signal-to-noise ratio (SNR) for elimination of noise, and the clutter-to-signal ratio (CSR), for elimination of the residual clutter. For the velocity, the signal qual-

ity index (SQI) is also used. This index is related to width of the velocity spectrum, and it is an indicator of targets within one measurement bin moving at different velocities.

## **Calibration, network monitoring and quality control**

A proper calibration of the weather radars is particularly important, when the data are used for quantitative precipitation estimates or when the data from several radars are combined together. Common calibration procedures remain as one of the most important goals of the NORDRAD community from the very beginning.

In the latter half of the 1990s, a significant difference in the reflectivity was found between the Swedish and Finnish radars. In studies within the NORDRAD collaboration in 1996–2003, the main causes for the discrepancy were successfully determined and removed. It originated mainly from two erroneously given constants in the settings of the signal processors, one causing overestimation in Sweden, another causing underestimation in Finland. For this study, several radars were calibrated using external microwave sources, feedhorns and reflective spheres (Koistinen *et al.* 1998) and methods for paired-radar analysis were developed and utilized (Huuskonen 2002).

Regular maintenance and calibration is essential for a network to achieve and maintain high data quality. At FMI, each radar is calibrated twice a year, both for the antenna pointing and power. The antenna pointing in azimuth is determined by using masts at known directions and observations of the Sun (Huuskonen and Holleman 2007). The antenna pointing in elevation is based on measuring the antenna position by the plumb-line method, and by observations of the Sun. The calibration of the received power is based on standard methods of measuring the power loss and using a signal generator as a reference. Tools provided by the radar software are utilized for this.

The antenna pointing and receiver stability are operationally monitored in between the scheduled maintenance, by using the Sun hits detected in the operational scans. This “online”

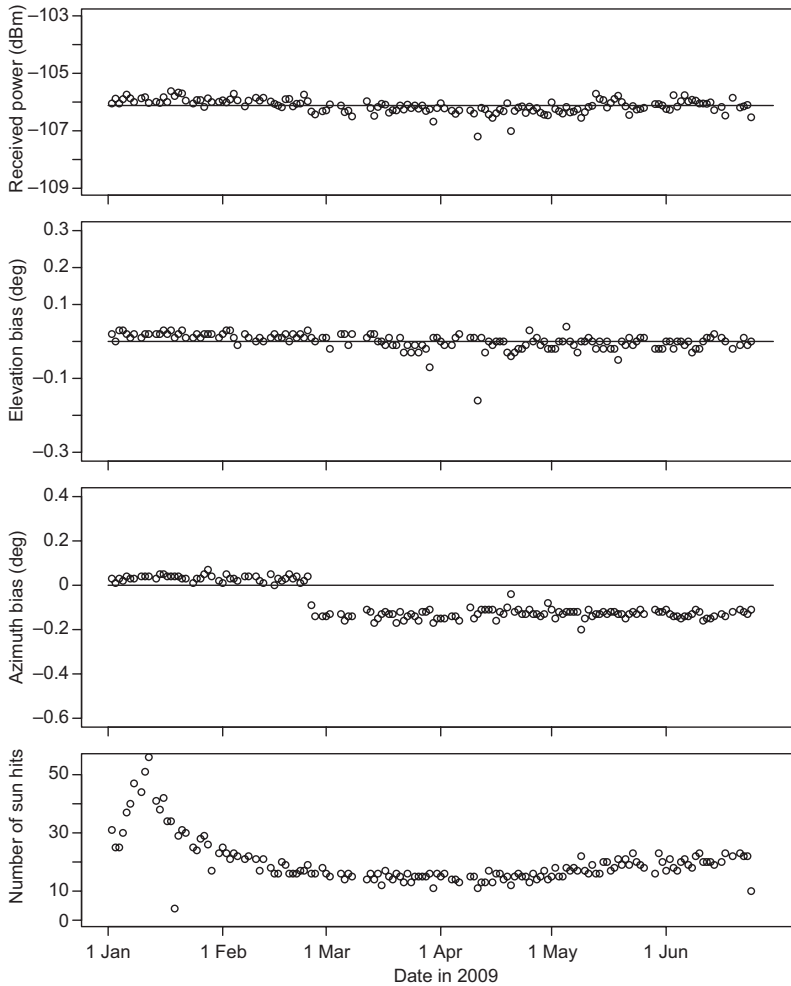


**Fig. 4.** The received power, bias in the antenna elevation and azimuth and the number of sun hits for the Vimpeli radar during January–April 2009. The horizontal lines indicate the mean power (top panel), and the zero antenna biases (second and third panels).

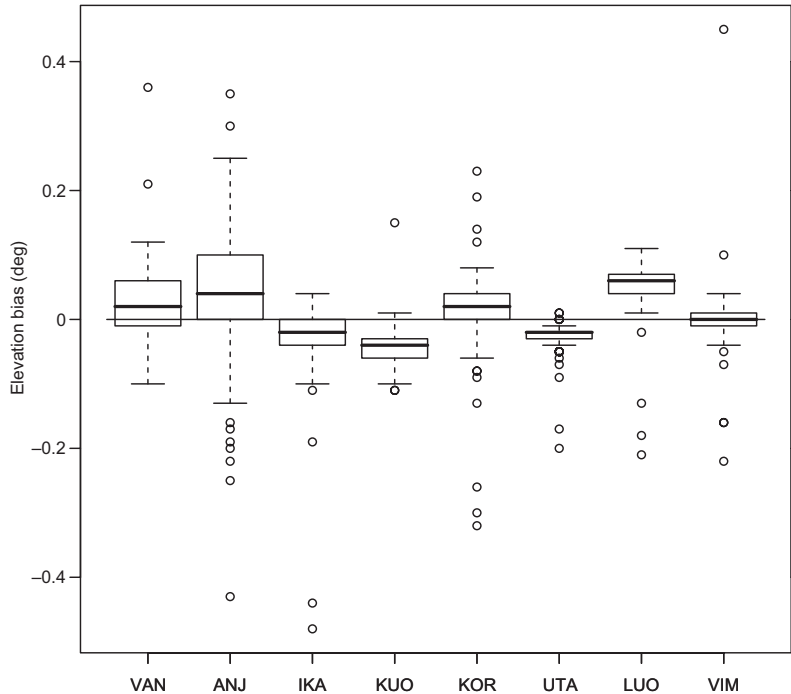
method is described by Huuskonen and Holleman (2007). In the method, use is made of the signals recorded by the radar whenever the antenna points close enough to the Sun. Typically, some tens of Sun hits are observed daily, which is sufficient to determine the antenna pointing, the power received from the Sun, as well as the width of the image of the Sun as seen by the radar.

The number of Sun hits (Fig. 4, bottom panel) is large just after the winter solstice when the sun climbs only a little above the horizon and thus stays for a long time at the lowest elevation angles of the radar. During the winter solstice the number is lower, because the sun does not hit the beam at higher angles at all. Towards the spring equinox the number of hits decreases as the sun traverses the lower angles faster. This figure indi-

cates that this method is especially well suited to higher latitudes; north of the polar circle there is an inevitable gap around the winter solstice. The results are based on data measured by the Vimpeli radar during January–April 2009.

The Sun measurements show, that the antenna system, as well as the radar receiver system, are very stable. The standard deviation of the elevation and azimuth angle biases is less than  $0.02^\circ$ , and that of the received power less than 0.2 dB. This scatter includes both the changes in the radar system itself as well as the scatter produced by the analysis method. Hence the stability of the antenna system and the receiver are even better than these numbers indicate. The azimuth bias shows a sudden change on 24 February 2009 when the antenna rotation direction was changed. The azimuth bias since

**Fig. 5.** The distribution of the antenna elevation bias for all radars of the FMI network during January–April 2009. The radar are shown in the order of installation starting from the oldest. For each radar, the median is shown with a thick line, the 1st and 3rd quartiles by a box. Whiskers indicate data points closer than 1.5 times the box length from the quartiles, and data points beyond that are marked with circles.



then is  $-0.12^\circ$ , which is high enough to be corrected during the annual maintenance.

The antenna pointing in elevation is especially crucial for the use of the radar data, because an error in the elevation produces an error in the altitude of the measurement. Statistics of the antenna elevation of the FMI network for January–April 2009 show that the elevation bias was less  $0.02^\circ$  in absolute value except for Luosto, where the bias was  $0.06^\circ$  (Fig. 5). The scatter of values, as indicated by the 1st and 3rd quartiles indicates that the older systems had a larger variation in elevation than the newer systems, which is as expected.

Data assimilation of the radar wind data into operational numerical weather prediction models (NWP) provides additional network monitoring tools. All conventional and many remote sensing weather observations are assimilated with the NWP model data. NWP model counterparts for the radial wind components can be computed from the NWP data using observation modelling (Järvinen *et al.* 2009) and inter-compared with the radar data (Salonen *et al.* 2007b). Bias estimation (Salonen *et al.* 2007a) of radial winds interfaces the radar data with all other atmos-

pheric observations and NWP model data. This provides an additional network monitoring tool, as the quality of the NWP wind data over the radar network is rather homogenous, while the quality of individual radars in the networks may vary. This monitoring tool is operationally available, as the FMI radar data is part of the observational input for the FMI NWP system (Salonen *et al.* 2009).

Radar wind data can also be processed to wind profiles (Weather Radar Wind Profiles, WRWP). Since 2003, the quality monitoring of the FMI WRWP has been provided for the Eumetnet WINPROF programme hosted by the UK Met Office (Parret *et al.* 2004). The monitoring is performed both monthly and quarterly, using statistics of radar wind differences from background winds, as given by the Met Office NWP model. The statistics include the bias and rms error for the wind components, as well as for wind direction and speed. The monitoring also includes similar statistics for a group of nearby radiosonde stations. This feedback has been very valuable in improving the quality of the wind profiles processed from the FMI radar data. The statistics in 2003 showed large random

errors, which were reduced considerably when low quality spurious winds were removed by tightening the quality control. At present, the radar wind profile quality is comparable to that of the radiosonde winds, except that below about 2 km a systematic negative bias is observed in the wind speed. This bias is caused most likely by radial velocities contaminated by ground clutter. Work is ongoing to remove this bias.

## Post-processing

A fraction of the clutter is immune to Doppler filtering because it originates from sources with true or apparent speeds exceeding the clutter filtering, such as interference, sea clutter and echoes from birds. It is removed in a fuzzy logics based post-processing procedure (Peura 2002, Koistinen *et al.* 2004). Related software has been operational since May 2002. The applied techniques involve recognition of graphical primitives (size, elongation, orientation, and steepness). In the filtering process, detection and removal are treated as separate processes. The original data are saved, and the removal is applied at different levels depending on the end user requirements.

All clutter-cancellation algorithms create small gaps in the data at bins, where small clutter targets such as masts are embedded in precipitation areas. Such gaps are filled by spatial interpolation from the neighbouring pixels. The effects of the clutter cancellation procedures are illustrated in Fig. 6.

For the end-user products, concentrating on precipitation near the ground level, a correction for vertical profile of reflectivity (VPR) is applied. The magnitude of the correction varies seasonally and with the distance from the nearest radar. In areas of good radar coverage, the correction seldom exceeds 5 dB (Koistinen *et al.* 2004).

The relation of radar reflectivity ( $Z$ ,  $\text{mm}^6 \text{m}^{-3}$ ) and the rainfall intensity ( $R$ ,  $\text{mm h}^{-1}$ ), the  $R(Z)$  relation is of primary interest for hydro-meteorological applications (e.g., Joss and Waldvogel 1990). The  $R(Z)$  relation is however very different for rain, snow, sleet, graupel, and their mixture, and varies spatially and temporally. Surface

observations of actual water phase of precipitation are available with much coarser spatial and temporal resolution (typically 50–100 km, 1–3 h) than radar observations (1 km, 5 min). Thus, an empirical equation is needed to determine the most likely water phase for each radar measurement bin. The selection of the relation to be used is based on the analyzed air temperature and humidity at the height of 2 m, and uses an empirical equation for the probability of water (PW), as presented by Koistinen and Saltikoff (1998)

$$PW = \frac{1}{1 + e^{22 - 2.7T - 0.2RH}}, \quad (1)$$

where  $T$  ( $^{\circ}\text{C}$ ) is the air temperature, and RH (%) is the relative humidity, both at the height of 2 metres. PW values range from 0 (snow) to 1 (rain) and the  $R(Z)$  relation is selected accordingly.

For rain ( $PW > 0.8$ ), the  $R(Z)$  equation by Dölling *et al.* (1998) is used. The snow equation, used when  $PW < 0.2$ , was originally based on Sekhon and Srivastava (1970), but it was adjusted based on gauge comparisons in 2005. Between the two limits, a linear fit between the two values is used. The  $R(Z)$  relations are given as

$$\begin{aligned} PW > 0.8: Z &= 316R^{1.5} \\ PW < 0.2: Z_e &= 100S^2. \end{aligned}$$

where  $S$  is the snowfall intensity ( $\text{mm h}^{-1}$ ),  $Z_e$  is the equivalent radar reflectivity factor, which differs from the cloud physical definition of  $Z$ , because the radar processor algorithm assumes dielectricity values valid for water, not for snow.

In most applications, data are used from more than one radar. Even if the measurements of one radar would cover the requested area, neighbouring radars often provide measurements closer to the surface of the Earth. Thus, the data from several radars is combined. In overlapping areas, several methods are available: one can for instance choose the value measured at lower altitude, the stronger value or average of the two values measured by individual radars. At FMI, an alternative method for generating radar composites from polar volume data has been developed. The method uses the data from the two lowest elevation angles and applies weighted

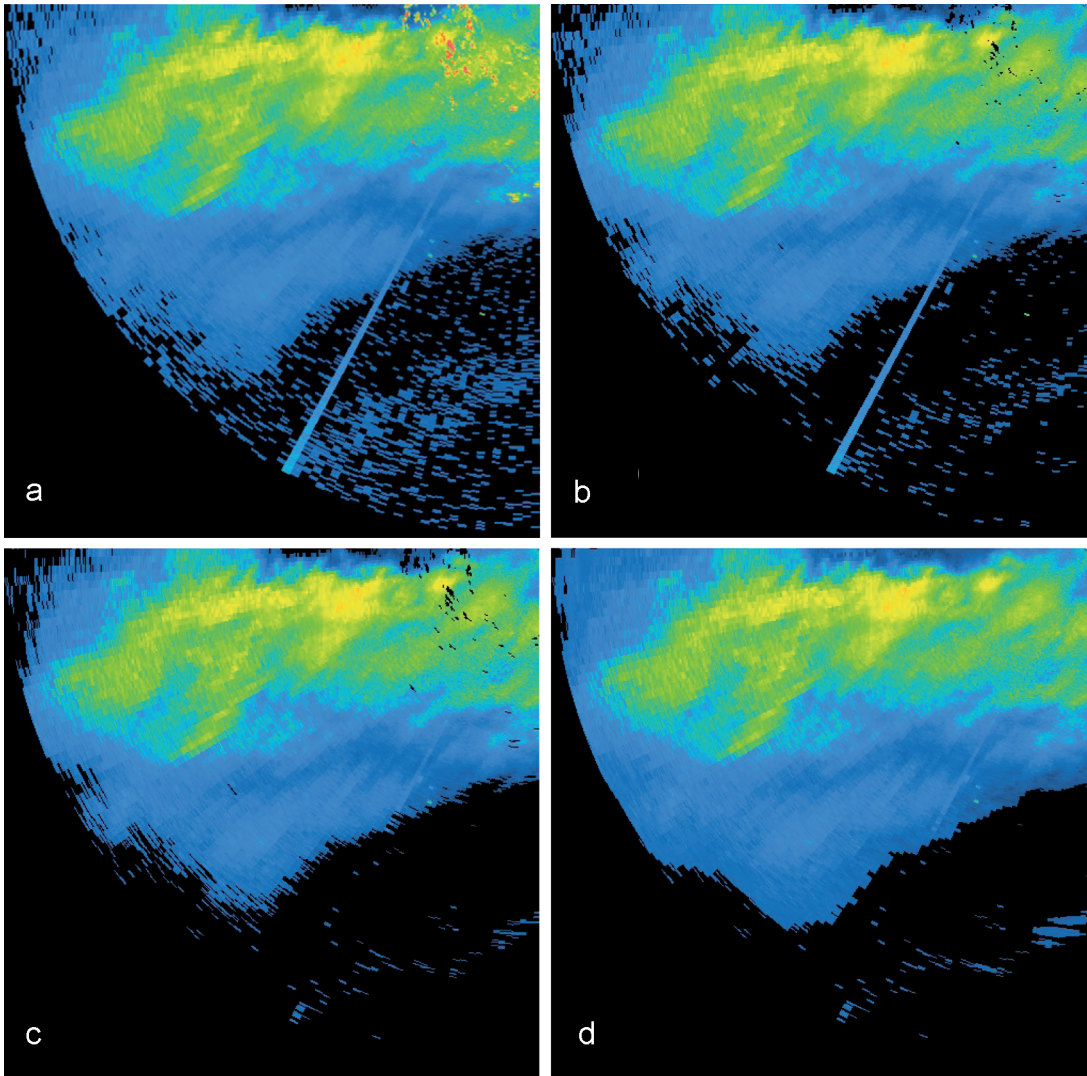


**Fig. 6.** The same sector PPI reflectivity at four phases of processing. The radar is located in the top right corner of each image, curving edge is 250 km from radar and the southwest-pointing ray is from the Sun: (a) Total reflectivity without Doppler filtering. Strong ground clutter near the radar and the interference from the Sun are clearly visible. (b) Reflectivity after Doppler filtering and thresholding at the signal processor. Thresholding has created gaps to the locations of the strongest ground clutter, and the Sun is still visible. (c) Reflectivity after the fuzzy-logics based post-processing procedure, which has successfully removed the effects of the Sun, and some of the residual noise or the clutter above the precipitating area near the lower edge of the image. (d) Reflectivity after the gap-filling procedure.

spatial interpolation to smooth measurement differences between neighboring radars.

### Remaining quality challenges

Challenges related to weather radars in northern Europe were discussed by the BALTEX (The Baltic Sea Experiment within the World Cli-

mate Research Program) working group, which produced a list of 16 challenges most relevant in northern Europe in the early 21st century (Saltikoff *et al.* 2004). The majority of these challenges have been solved for Finland at a satisfactory level either by a careful design of the network and the antenna scanning strategy, or by the post-processing described above (*see* Table 5). Some of the challenges are not as

demanding in Finland as in some other countries e.g. due to topography. Others are already corrected operationally. For example, Doppler filtering was originally not at its optimal level in some of the countries participating in the query. For some other solutions, the algorithm has been selected but not yet implemented operationally. For instance, the solutions related to dual polarization will become available gradually with the upgrades of the radar networks. For the remaining two challenges, research is still ongoing.

In Finland, the largest remaining challenges are the overhanging precipitation, the total beam overshooting and the sea clutter. The overhanging precipitation is related to such precipitation which is correctly measured aloft but evaporates before reaching the ground. This is most typical in association with warm fronts. Due to the three-dimensional structure of the frontal precipitation band, correction using vertical profile of reflectivity is difficult or impossible. Attempts to identify and eliminate the overhanging precipitation by using the NWP data have been made (Pohjola and Koistinen 2004) but the results were not satisfactory mainly due to prediction errors related to the timing of the precipitation bands in the model. Total beam overshooting occurs when the precipitation top does not extend to the height of the lowest radar measurement. This is typically associated with drizzle and snowfall, and espe-

cially to snow fall in a cold climate. For the total beam overshooting, there is no obvious solution, even though the situation has been improved significantly with the completion of the FMI radar network by the Vimpeli radar in 2005. Sea clutter occurs when the microwaves are channeled to the sea surface either directly or due to anomalous propagation conditions in the atmosphere, and are reflected from the surface waves at sea. As the sea waves move with non-zero radial velocities, Doppler filtering can not remove these echoes.

### Processing from data to products

The radar data are processed centrally to the largest extent possible. Data are collected on the radar sites, transmitted to FMI HQ, processed to different products and images and transmitted to forecasters at FMI local units in four different cities as well as thousands of external customers and other end-users.

The data transmission speed from radars to HQ and to the users has been increased over the years. The first radars used the speed of  $19.2 \text{ Kb s}^{-1}$ , which was so slow that it limited the number of saved parameters and the measurement resolution. The measurements and the clutter cancellation were made with a higher resolution, but the resolution was decreased by

**Table 5.** Challenges in the northern European radars as listed by the BALTRAD in 2003, and the FMI actions and plans.

Challenge	Action	Status
Radar siting	Design and experience	Not a problem in Finland
Beam blockage	Siting	Not a problem in Finland
Scan strategy	Compromizes	Continuing work due to changing needs of data users
Ground clutter	Doppler	Operational
AP clutter	Doppler	Operational
Vertical dBZ profile	Correction	Operational
Data assimilation to models	Task change	Operational
Nowcasting tools, automatic detection of phenomena	Tasks, dualpol, algorithms	Operational
Total beam overshooting	More radars	Operational
$R, S(Z_e)$	$T + RH$ analysis	Operational
Suboptimal compositing algorithms	New algorithms	Operational
Gauge adjustment	Kriging	Partially operational
Attenuation by precipitation	Dual pol corr.	To be implemented
Water phase	Dual pol	To be implemented
Overhanging precipitation	Data fusion, compositing algorithms	Ongoing research
Sea clutter	Dual polarization	Ongoing research

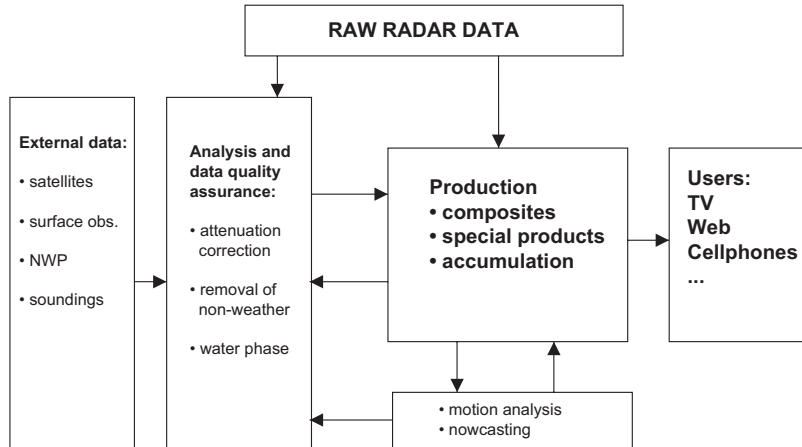


**Fig. 7.** Processing chains — forming a processing net — for the radar data.

averaging the processed data before transmission. Parameters such as the total reflectivity and the Doppler spectrum width were not saved. The data transmission speed grew gradually to 64 Kbps in 1996, then to 128 Kbps and finally to 256 Kbps in 2002. With the upgrade to dual polarization radars in 2009, the connection to the Vantaa radar was upgraded to 2 Mbps in May 2009, which is a hundred fold increase over the initial speed of the previous generation radars

The radar data production is no longer just a simple processing chain of cleaning and tuning the data coming from the radar. Rather, data from external data sources such as temperatures from NWP models are used in several phases of the process. The order in which the corrections are performed, affects the result, and some corrections are applied recursively. The processing chains form currently a network of modules (Fig. 7).

## Applications

### Automated nowcasting

The method of predicting precipitation for the next few hours, developed at FMI, applies a modified correlation-based atmospheric motion vector (AMV) system developed by the EUMETSAT (Holmlund 1998). Radar reflectivity fields from the height of 500 m with the interval of 5 minutes are used as an input to the AMV system. The system provides a smooth vector field from which a trajectory field is calculated. Speed and direc-

tion inaccuracies along the trajectories provide an “error ellipse” around each starting point of a trajectory. The reflectivities within the ellipse are then applied to calculate a set of forecast products for the interval of 0.5–4 hours from the initial time (Hohti *et al.* 2000, Koistinen *et al.* 2004).

This method can successfully be applied only to a homogenous and clean field of reflectivity which is wide enough: if we assume that precipitation areas move  $50 \text{ km h}^{-1}$ , a two-hour forecast requires at least 100 km coverage around the area of interest. Using a single radar for extrapolation fails, because the precipitation can emerge from outside of a single radar image. This aspect is especially important in a climate of transient low pressure systems, which dominate the rain events over the local convection.

From the perspective of nowcasting, the most harmful errors are due to the residual clutter echoes from moving targets such as ships. If they occur near precipitation areas, smoothing can be used to reduce their effect in the motion vector field, but during clear weather, such a compensation method is not possible.

### Forest fire index

The FMI calculates a forest fire index (FFI) to alert authorities and the general public about the potential risk for forest fires. The goal is to reduce the number and spread of forest fires and to reduce the delay in fire control activities by focusing control flights in the areas at risk. In the FFI system, the volumetric moisture

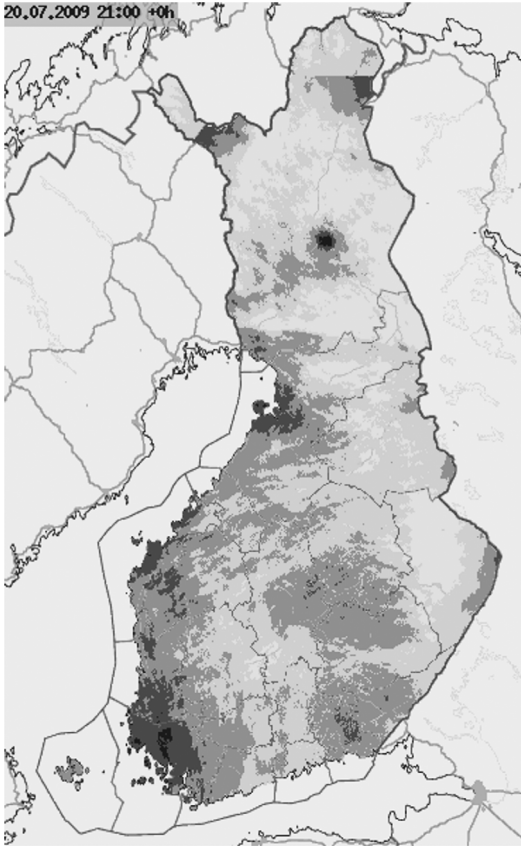


**Fig. 8.** An example of the forest fire index for 20 July 2009. The dark greys represent the areas with higher risk. The map shows well the drier climate near the west coast, as well as an artificial dry spot over the Luosto radar (due to a radar hardware problem).

content of a 6-cm-thick surface layer (“fuel layer”) is estimated from weather observations using a semi-empirical model developed for this purpose (Heikinheimo *et al.* 1998, Venäläinen and Heikinheimo 2003, Tanskanen and Venäläinen 2008). The calculated volumetric moisture values are then scaled to index values from 1 to 6 based on long term climate records.

In the FFI model, the surface layer humidity depends on evaporation and precipitation of the previous days. The radar data are used as accumulated 3-h precipitation values. Reflectivity measurements are first built in to a low altitude nation-wide composite, and these data are used as a basis for the accumulations. Since 2005, rain gauge data have been used only in the areas of poor radar coverage in the north and western archipelago (A. Venäläinen and P. Junila

pers. comm.). The evaporation is estimated from weather station data for the same 3-h period. The estimate of the soil moisture is increased or decreased with the sum of evaporation and precipitation.

When the model was first taken into use, the forest fire index was calculated for individual stations. In the 1980s, it was noticed, that single station indices are not representative for forest fire warnings to entire counties. To obtain estimates of drought between stations, the Kriging analysis (e.g. Bigg 1991) in a grid interval of 10 km was used (Heikinheimo *et al.* 1998). In 2008, the resolution was increased to 1 km which was largely due to the increased confidence in quantitative radar estimates of precipitation. The added resolution is essential for the recognition of the small scale permanent differences in the areas of sharp gradients in precipitation patterns due to meso-scale phenomena, such as the lake and sea breeze.

However, using radar without rain gauge adjustment and in fine resolution, poses huge demands for quality assurance. A bias may lead to unnatural drying or moistening of the forests, as it is accumulated and compared with evaporation data for other sources. This in turn may cause too many or too few warnings. Even an error source which may be small in single images such as the partial beam blocking, becomes visible in longer accumulations. Residual ground clutter may cause “wet spots” while too strong clutter cancellation causes “dry spots”.

Even with these shortcomings, the forest fire warning product is used as a guidance to the meteorologist in duty, but the final decision of accepting or rejecting the suggested warning is made by the meteorologist. The maps on index (Fig. 8) are also distributed as additional background information to other authorities involved in the forest fire prevention (A. Venäläinen pers. comm.).

## Summary, discussion and future outlook

This paper provides a description of the Doppler radar network of the Finnish Meteorological Institute. The network operates in a favourable topographical area and in a relatively cold cli-

mate, where the precipitation is often shallow and related to extratropical cyclones.

After the installation of the Vimpeli radar in 2005, the network has finally reached its planned coverage. There are still some areas in the north and east, which are poorly covered especially for shallow precipitation in winter.

The oldest radars in the network have reached 15 years of age, and the process of replacing these radars has already started. Signs of mechanical wearing are visible, and some spare parts are in short supply. New technologies and methods have become available during the lifetime of the network, such as more advanced processing and dual polarization applications.

The use of the radar data has increased over the years, but still the most important applications are within hydro-meteorology, weather forecasting, aviation and road maintenance. The demand for the radar data in hydrological applications (e.g. river discharge modeling) is ever increasing, with the improving quantitative accuracy of the radar data. Also, data assimilation of Doppler winds in numerical weather prediction models has become operational. The next development phase will be the gradual introduction of dual-polarization radars in the network. This innovation will certainly bring forward new applications and products, but it will take a number of years before their full capability is utilized. This is more than well proved by the use of the present Doppler radar network, the full benefits of which are only now being taken into use, some 15 years after the network building first begun.

*Acknowledgements:* The authors thank all members of the FMI weather radar team who contributed during the successful building of the radar network. Special thanks are due to Irene Suomi for her insight into forest fires.

## References

- Battan L.J. 1973. *Radar observation of the atmosphere*. The University of Chicago Press, Chicago and London.
- Bigg G.R. 1991. Kriging and interregional rainfall variability in England. *Int. J. Climatol.* 11: 663–675.
- Bringi V.N. & Chandrasekar V. 2001. *Polarimetric Doppler weather radar*. Cambridge University Press, Cambridge, United Kingdom.
- Carlsson I. 1994. Nordrad — weather radar network. In: Collier C.G. (ed.), *COST75 Weather radar systems International seminar Brussels, Belgium*. Report EUR 16013-COST 75, ECSC-EEC-EAEC, Bruxelles, Luxembourg, pp. 45–52.
- Dölling I., Joss J. & Riedl J. 1998. Systematic variations of Z-R relationships from drop size distributions measured in northern Germany during seven years. *Atmos. Res.* 48: 635–649.
- Doviak R.J. & Zrnic D. 1993. *Doppler radar and weather observations* (2nd ed.). Academic Press, San Diego.
- Heikinheimo M., Venäläinen A. & Tourula T. 1998. A soil moisture index for the assessment of forest fire risk in the boreal zone. In: Dalezios N.R. (ed.), *Proceedings of the International Symposium on Applied Agrometeorology and Agroclimatology, Volos, Greece, 24–26 April 1996*, EUR 18328-COST 77, 79, 711, European Commission, Belgium, pp. 549–556.
- Hohti H., Koistinen J., Nurmi P., Saltikoff E. & Holmlund K. 2000. Precipitation nowcasting using radar-derived atmospheric motion vectors. *Physics and Chemistry of the Earth, Part B: Hydrology, Oceans and Atmosphere* 25: 1323–1327.
- Holmlund K. 1998. The utilization of statistical properties of satellite-derived atmospheric motion vectors to derive quality indicators. *Weather Forecasting* 13: 1093–1104.
- Huuskonen A. 2002. A method for monitoring the calibration and pointing accuracy of a radar network. In: *Proceedings of 30th AMS Conference on Radar Meteorology, Munich, Germany, July 18–24, 2001*. Amer. Meteor. Soc., Boston, pp. 29–31.
- Huuskonen A. & Holleman I. 2007. Determining weather radar antenna pointing using signals detected from the sun at low antenna elevations. *J. Atmos. Oceanic Technol.* 24: 476–483.
- Joe P. & May P. 2003. Correction of dual PRF velocity errors for operational Doppler weather radars. *J. Atmos. Oceanic Technol.* 20: 429–442.
- Joss J. & Waldvogel A. 1990. Precipitation measurement and Hydrology. In: Atlas D. (ed.), *Radar in meteorology*, Amer. Meteor. Soc., Boston, pp. 577–606.
- Järvinen H., Salonen K., Lindskog M., Huuskonen A., Niemelä S. & Eresmaa R. 2009. Doppler radar radial winds in HIRLAM. Part I: observation modelling and validation. *Tellus* 61A: 278–287.
- Kaipio J.P. & Somersalo E. 2005. *Statistical and computational inverse problems*. Applied Mathematical Sciences 160, Springer Science + Business Media, Inc.
- King R. 1989. Operational experiences with the Finnish Weather radar network. In: Collier C.G. & Chapuis M. (eds.), *Weather Radar networking. Seminar on COST Project 73*, Kluwer Academic Publishers, Dordrecht, Boston, London, pp. 91–101.
- Koistinen J. & Saltikoff E. 1998. Experience on customer products of accumulated snow, sleet and rain. In: Collier C.G. (ed.), *Advanced weather radar systems, COST 75, International seminar, Locarno, Switzerland*, Office for Official Publications of the European Communities, Luxembourg, pp. 397–406.
- Koistinen J., Saltikoff E., King R. & Harju A. 1998. Monitoring and assessment of systematic measurement errors in the NORDRAD. In: Collier C.G. (ed.), *Advanced*

- weather radar systems, *COST 75, International seminar, Locarno, Switzerland*, Office for Official Publications of the European Communities, Luxembourg, pp. 62–67.
- Koistinen J., Michelson D.B., Hohti H. & Peura M. 2004. Operational Measurement of precipitation in Cold Climates. In: Meischner P. (ed.), *Weather radar*, Springer-Verlag Berlin, Heidelberg, New York, pp. 78–110.
- Parrett C.A., Turp M., MacPherson B. & Oakley T. 2004. Quality monitoring of weather radar wind profiles at the Met Office. In: *Proceedings of ERAD 2004*, ERAD Publication Series 2, Copernicus GmbH, Göttingen, pp. 168–173.
- Passarelli R., Romanik P., Geotis S.G. & Siggia A.D. 1981. Ground clutter rejection in the frequency domain. In: *Preprints, 20th Conf. on Radar Meteorology*, Boston, MA, Amer. Meteor. Soc., Boston, pp. 308–313.
- Peura M. 2002. Computer vision methods for anomaly removal. In: *Second European Conference on Radar Meteorology, Delft University of Technology, 18–22 November 2002, Delft, the Netherlands*, ERAD Publication Series vol. 1, Copernicus GmbH, Göttingen, pp. 312–317.
- Pirttilä J., Lehtinen M., Huuskonen A. & Markkanen M. 2005. A proposed solution to the range-Doppler dilemma of weather radar measurements by using the SMPRF codes, practical results and a comparison to operational measurements. *J. Appl. Meteor.* 44: 1375–1390.
- Pohjola H. & Koistinen J. 2004. Identification and elimination of overhanging precipitation. In: *Proceedings of 3rd European Conference on Radar Meteorology and Hydrology (ERAD), 6–10 September 2004, Visby, Sweden*, vol. 2, Copernicus GmbH, Göttingen, pp. 91–93.
- Rinehart R.E. 1997. *Radar for meteorologists* (3rd ed.). Rinehart Publications, Grand Forks, ND, USA.
- Salonen K., Järvinen H., Eresmaa R. & Niemelä S. 2007a. Bias estimation of Doppler radar radial wind observations. *Q. J. R. Meteor. Soc.* 133: 1501–1507.
- Salonen K., Järvinen H., Järvenoja S., Niemelä S. & Eresmaa R. 2007b. Doppler radar radial wind data in NWP model validation. *Met. Appl.* 15: 97–102.
- Salonen K., Järvinen H., Haase G., Niemelä S. & Eresmaa R. 2009. Doppler radar radial winds in HIRLAM. Part II: optimizing the super-observation processing. *Tellus* 61A: 288–295.
- Saltikoff E., Gjertsen U., Michelson D.B., Holleman I., Seltmann J., Odakivi K., Huuskonen A., Hohti H., Koistinen J., Pohjola H. & Haase G. 2004. Radar data quality issues in northern Europe. In: *Proceedings of ERAD 2004*, ERAD Publication Series 2, Copernicus GmbH, Göttingen, pp. 212–215.
- Sekhon R. & Srivastava R. 1970. Snow size spectra and radar reflectivity. *J. Atmos. Sci.* 27: 299–307.
- Serafin R.J. & Wilson J.W. 2000. Operational weather radar in the United States: progress and opportunity. *Bull. Am. Met. Soc.* 81: 501–518.
- Sigmat 1997a. *IRIS software user's manual*. Sigmet Inc., Westford, MA, USA.
- Sigmat 1997b. *RVP 6 Doppler signal processor user's manual*. Sigmet Inc., Westford, MA, USA.
- Tabary P. 2007. The new French operational radar rainfall product, part I: methodology. *Weather Forecasting* 22: 393–408.
- Tanskanen H. & Venäläinen A. 2008. The relationship between fire activity and fire weather indices at different stages of the growing season in Finland. *Boreal Env. Res.* 13: 285–302.
- Venäläinen A. & Heikinheimo M. 2003. The Finnish forest fire index calculation system. In: Zschau J. & Kuppers A. (eds.), *Early warning systems for natural disasters reduction*, Springer Verlag, Berlin, pp. 645–648.
- Waldteufel P. & Corbin H. 1979. On the analysis of single-Doppler radar data. *J. Appl. Met.* 18: 532–542.
- WMO 2006. *Guide to meteorological instruments and methods of observation* no. 8 (7th ed.). Secretariat WMO, Geneva, Switzerland.